

Reweighting of visuomotor areas during motor processing subsequent to somatosensory cortical damage



Yuqi Liu ^{a,b,*}, Elizabeth J. Halfen ^c, Jeffrey M. Yau ^c, Simon Fischer-Baum ^d, Peter J. Kohler ^{e,h}, Olufunsho Faseyitan ^f, H. Branch Coslett ^f, Jared Medina ^{b,g,*}

^a CAS Center for Excellence in Brain Science and Intelligence Technology, Chinese Academy of Sciences, PR China

^b Department of Psychological and Brain Sciences, University of Delaware, USA

^c Department of Neuroscience, Baylor College of Medicine, USA

^d Department of Psychological Sciences, Rice University, USA

^e Centre for Vision Research, York University, Canada

^f Department of Neurology, University of Pennsylvania, USA

^g Department of Psychology, Emory University, USA

^h Department of Psychology, York University, Canada

ARTICLE INFO

Keywords:

Brain reorganization
Brain damage
Sensorimotor integration
Somatosensory cortex
Motor cortex
Visuomotor

ABSTRACT

Somatosensory inputs are critical to motor control. Animal studies have shown that primary somatosensory lesions cause sensorimotor deficits along with disrupted organization in primary motor cortex (M1). How does damage in primary somatosensory cortex (S1) influence motor networks in humans? Using fMRI, we examined two individuals, LS and RF, who had extensive damage to left somatosensory cortex, but primarily intact motor cortex and preserved motor abilities. Given left S1 damage, tactile detection and localization were impaired for the contralateral hand in both individuals. When moving the contralateral hand, LS, with near complete damage to S1 hand area, showed increased activation in ipsilesional putamen and deactivation in contralateral cerebellum relative to age-matched controls. These findings demonstrate influences of S1 damage to subcortical sensorimotor areas that are distant from the lesion site, and a potential reweighting of the motor network with increased action selection in putamen and inhibition of sensory prediction in cerebellum in the face of sensory loss. In contrast, RF, who had a small island of spared S1 in the hand area, showed greater activation in contralateral S1 for movement versus rest. This same region was also activated by pure somatosensory stimulation in a second experiment, suggesting that the spared S1 area in RF still subserves sensorimotor processing. Finally, the right middle occipital gyrus was more strongly activated in both individuals compared with controls, suggesting the potential reliance on visual imagery in the face of degraded sensory feedback.

1. Introduction

Successful hand actions critically depend on somatosensory feedback that informs the current state of the hand and the object. Integration of sensory information into motor commands relies on the communication between sensory and motor networks. The adjacent primary motor cortex (M1) and primary somatosensory cortex (S1) are densely interconnected and instantiate such communication (Catani et al., 2012; Ghosh and Porter, 1988; Mao et al., 2011; Porter and White, 1983; Tamé et al., 2015). Although simple tactile detection could be relearned (La Motte and Mountcastle, 1979), lesions in S1 profoundly influence motor processing, reducing the power, dexterity and use of the contralateral

hand in animals (Ghosh and Porter, 1988; Mathis et al., 2017; Xerri et al., 1998), humans (Carey et al., 2018; Chen et al., 2006; Jeannerod et al., 1984), and preventing learning of new motor skills (Pavlides et al., 1993). Infarcts in S1 have altered response profiles (Kambi et al., 2011; Kato and Izumiya, 2015; Qi et al., 2010) and organization in M1 (Harrison et al., 2013). These findings provide evidence for reorganization of the primary motor cortex due to primary somatosensory damage.

Beyond primary motor cortex, motor networks encompass a wide range of cortical and subcortical areas. By asking participants to perform simple flexion-extension or finger-tapping movements, studies report robust activation in bilateral premotor cortex, supplementary motor

* Corresponding authors.

E-mail addresses: liuyq@ion.ac.cn (Y. Liu), jared.medina@emory.edu (J. Medina).

area (SMA), posterior parietal activation (PPC), and subcortically in basal ganglia, thalamus, and cerebellum (Eickhoff et al., 2009; Hardwick et al., 2018). Similar paradigms have been used in brain-damaged individuals to study somatosensory and motor reorganization after stroke. In these studies, stroke survivors performed simple whole-hand opening-closing/gripping or finger tapping movements and their motor activation was compared between the two hands or with neurologically-typical groups (Carey et al., 2002, 2006; Grefkes and Ward, 2014; Ward et al., 2003). By correlating motor activity with hand function, researchers were able to infer neural correlates of functional recovery while accounting for various factors such as lesion location and size (Grefkes and Ward, 2014; Grefkes and Fink, 2011).

One dimension along which motor areas vary functionally is the degree they participate in sensorimotor integration. For example, the cerebellum has been proposed to be critical for predicting sensory consequences during movement, and disrupting projections from S1 to cerebellum impairs motor performance in rats (Jenkinson and Glickstein, 2000). Neuroimaging studies reported increased cerebellar activity when participants traced line drawings versus drawing freely (Jueptner et al., 1996) and when the expected touch from one's own action was experimentally delayed (Blakemore et al., 2001). Recent studies established a double-dissociation between M1 and basal ganglia such that lesioning rats' M1 affected the execution of visually-guided but not overly learned motor sequences, whereas damaging the basal ganglia impaired overtrained but not visually-guided motor sequences (Mizes et al., 2023a, 2023b). These findings suggest that M1 is required for integrating sensory information while the basal ganglia are essential for executing automatic, internally-generated kinematic patterns. One ramification of differential involvement in sensory processing is that each motor area may respond differently to damage in somatosensory cortex. However, the influence of somatosensory damage on motor networks in humans remains largely unknown.

The involvement of S1 in motor processing has been difficult to examine in humans. Given brain vasculature, most strokes that damage S1 also lead to M1 damage. We examined two individuals with extensive damage to left somatosensory cortex, but largely intact motor cortex. Both individuals demonstrated impaired tactile detection and localization with preserved motor abilities on the contralateral hand, providing a unique opportunity to investigate the reorganization of motor networks subsequent to somatosensory damage. Importantly, the two individuals differ in the extent of damage to the hand area of S1, with one individual (LS) having near complete damage and the other (RF) having a spared strip of S1 hand area along the central sulcus. These cases allow us to examine motor reorganization subsequent to somatosensory damage as well as the impact of the extent of the lesion.

We conducted an fMRI experiment in which LS and RF, along with eight age-matched controls, performed finger flexion-extension movements with each hand. Whole-brain comparisons between each brain-

damaged individual and the control group were performed to examine changes in the activation pattern of motor networks as a result of somatosensory damage. In addition, to separate sensory processing from motor control, LS and RF participated in a second fMRI experiment where they passively received tactile stimulation. This experiment allowed us to examine whether the spared portion of S1 hand area in RF had remaining sensory function, and the causal role of S1 damage in higher-level somatosensory areas in LS.

2. Materials and methods

2.1. Participants

At the time of testing, LS was a 63-year-old male who suffered a left hemisphere infarct that extended from the central sulcus posteriorly to superior temporal sulcus (Fig. 1A), affecting most of the lateral S1, part of S2, and inferior and superior parietal lobe. Upon observation, LS demonstrated clear deficits in touch and proprioception without vision, and heavily relied on visual information for moving the contralateral right hand. Precise manual tasks with vision (e.g., picking up a coin) were also difficult. He was clearly able to perform simple hand movements (e.g., opening and closing the fist) both with and without vision.

RF was a 49-year-old female (five years post-stroke) whose lesion, caused by an ischemic stroke, extended from the postcentral gyrus to superior temporal sulcus along with extensive damage to left parietal operculum, superior temporal gyrus, insula, inferior and middle frontal gyrus (Fig. 1B). Critically, there was spared tissue in the anterior bank of the postcentral gyrus in RF, leaving the most anterior part of the hand area in S1 intact (Fig. 1B). As with LS, RF relied heavily on vision for moving the contralateral right hand, yet showed no noticeable movement deficit.

For the motor neuroimaging experiment, we tested eight age-matched neurologically typical control participants (all right-handed, mean age = 61.5 years, SD = 7.9 years, 4 females). All research was approved by the IRBs of Baylor College of Medicine (RF), University of Delaware (LS, controls) and University of Pennsylvania (LS), with all participants providing written informed consent.

2.2. Experimental design

2.2.1. Behavioral testing

Tactile detection was examined using a weighted 1-down 1-up staircase procedure (10 planned reversals for LS, 20 for RF) with Semmes-Weinstein monofilaments (North Coast Medical Inc., CA, USA, 20 monofilaments for LS ranging from 0.008 g to 300 g; 5 monofilaments for RF ranging from 0.07 g to 300 g). The participant was seated with the tested hand resting on the table, palm facing up, with monofilaments presented to the middle fingertip with the patient's eyes

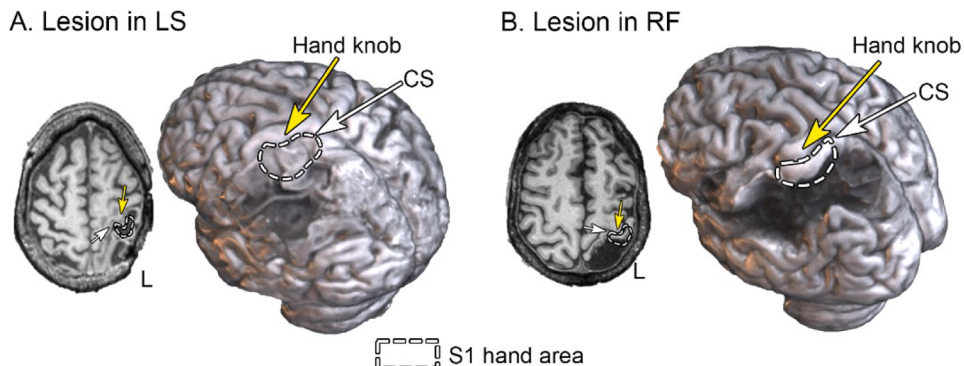


Fig. 1. Lesion location in LS and RF shown in one transversal slice and a rendered 3D brain based on T1-weighted MRI scans. The yellow arrows point to the hand knob in M1, the white arrows point to the central sulcus, and the dotted white outlines depict the estimated S1 hand area. Whereas LS had near complete damage to the hand area in S1, RF had an anterior portion spared. A detailed presentation of the lesions is shown in Figure S1.

closed. Starting from the heaviest filament, if the participant reported feeling the touch, the filament two levels lighter was used on the next trial, otherwise the filament one level heavier was used. Catch trials in which the experimenter approached the hand without touching were randomly interspersed in each block (approximately 1 out of 6 trials).

Tactile localization was assessed using a clearly suprathreshold monofilament using the method in Rapp et al., 2002 (300 g on the contralateral hand of both LS and RF; 1 g and 300 g on the ipsilateral hand of LS and RF respectively, four filaments above the threshold in both cases). The participant was seated with the tested hand resting on the table, palm facing down. In each trial the experimenter touched one of 22 pre-determined locations on the hand dorsum (Figure S2A) with the participant's eyes closed. Then the patient opened their eyes and pointed with the other hand where they felt touch on the tested hand. A second experimenter coded their response on a standard hand template. Each hand was tested in two blocks with one trial per location in randomized order. Hand order was balanced in ABBA manner.

An additional assessment of proprioception was performed with LS with the tested hand placed on a slider on a table. The hand and slider were covered under a white board. We instructed LS to rest the tested hand on the slider without making any voluntary movements. In each trial, the experimenter moved the slider to align LS's middle finger with one of the 15 locations (arranged in a grid of 30 cm wide and 16 cm deep, aligned with the body midline, Figure S2B) under the white board. Then LS pointed to a location on the white board directly above the perceived middle fingertip location using the untested hand. A picture of each judgment was taken and later compared with the actual target location. Each location was tested once in each block. Each hand was tested in two blocks in an R-L-L-R order.

2.2.2. Motor fMRI

LS, RF, and eight age-matched controls participated in the motor fMRI experiment in which a block-design was adopted (Grefkes et al., 2008; Jaillard et al., 2005). Each run began with a baseline period of six seconds, then alternated between 12 s of movement and 12 s of rest for 10 cycles, totaling 246 s. In hand movement phases, the monitor, viewed from a mirror mounted on the head coil, flashed the word "open" and "close" at 0.5 Hz and the participant opened and closed the tested hand accordingly. A central fixation cross was presented during rest. LS and controls ran three runs on each hand, RF ran two runs (due to time constraints) on each hand in an ABBA(AB) manner. Compliance with instructions was visually monitored during testing; all participants were easily able to complete the task.

2.2.3. Visual control fMRI

During the motor fMRI experiment, participants viewed the words "open" and "close" during hand movement versus a fixation cross during rest, raising the possibility that motor activation was driven by viewing words. To examine the effect of word presentation alone, control participants performed two runs of a visual experiment in which they passively viewed the same visual presentation as in the motor experiment (i.e. 12-seconds of word presentation, 12-seconds of fixation cross) while no hand movements were made. Seven out of the eight controls participated in this experiment. One control participant did not complete this experiment due to time constraints.

2.2.4. Somatosensory fMRI

Each run began with a baseline period of six seconds, then alternated between 30 s of tactile stimulation and 30 s of rest for four cycles, totaling 246 s. During the experiment, the participant rested their hands on each side of the body, palms facing up. An experimenter manually stroked the palm with a brush at 2 Hz frequency following a metronome presented via headphones that was only heard by the experimenter. The patient was instructed not to make any body movements and to fixate at a central cross on the monitor. Five runs were completed with LS (three contralateral, two ipsilateral), and four runs were completed with RF

(two contralateral, two ipsilateral) in an ABBA(A) manner.

2.3. MRI acquisition

LS's neuroimaging data were acquired from a Siemens Tim Trio 3T scanner at the University of Pennsylvania. A structural image was collected using a T1-weighted MPRAGE sequence (TR=1620 ms, TE=3.08 ms, flip angle = 15°, 192×256×160 voxels, 1 mm isotropic, FoV=19.2 × 25.6 cm). Functional MRI images were collected using a T2*-weighted echoplanar imaging (EPI) sequence (TR=3000 ms, TE=30 ms, flip angle=90°, 64×64×48 voxels, 3 mm isotropic).

Control participants were scanned using the same T1-weighted MPRAGE and T2*-weighted EPI sequences as with LS. Imaging data were obtained from a Siemens Prisma 3T scanner at the Center for Biomedical and Brain Imaging (CBBI) at the University of Delaware.

Imaging data from RF were obtained from a Siemens Prisma 3T scanner at the Center for Advanced MRI (CAMRI) at Baylor College of Medicine. A 3D anatomical scan was acquired using a T1-weighted MPRAGE sequence (TR=2300 ms, TE=2.98 ms, flip angle = 9°, 168×237×200 voxels (1 mm isotropic)). Functional MRI volumes were collected using a T2*-weighted echoplanar imaging (EPI) sequence (TR=1500 ms, TE=33 ms, flip angle=90°, 96×96×69 voxels, 2 mm isotropic).

2.4. fMRI preprocessing

Neuroimaging data were preprocessed in FSL 6.0 (FMRIB's Software Library). Preprocessing of functional scans involved removal of the first two volumes, high-pass filtering (cutoff at 100 s), slice-timing correction, spatial smoothing with 4 mm full width at half maximum (FWHM), and motion correction through 6-degrees-of-freedom (DOF) rigid-body transformation to the middle volume. Head motion was within 1 mm across all runs of all participants. T1-weighted structural images were brain-extracted with BET for controls and with optiBET (Lutkenhoff et al., 2014) for LS and RF. Brain-extracted T1-weighted images were then segmented into white matter, cerebrospinal fluid (CSF), and gray matter using FAST. Functional images were co-registered to brain-extracted structural images using 6-DOF transformation in FLIRT. Structural images were co-registered to the MNI152 template brain (1 mm isotropic) using 12-DOF transformation in FLIRT for controls and using the LINDA package for LS and RF implemented in R (v4.1.1; Pustina et al., 2016). Finally, we reconstructed surface space for the MNI152 template brain in FreeSurfer (7.2.0) and projected results from volumetric to surface space for visualization.

Assessing BOLD time course in LS and RF

Brain damage induced by stroke is known to alter the shape of the hemodynamic response, at times causing a delay in perilesional brain regions (Amemiya et al., 2012; Bonakdarpour et al., 2007). In this case, the standard hemodynamic response function (HRF) would not accurately model the brain response. To assess the time course of the HRF in LS and RF, we performed a whole-brain lag analysis in each individual under each task as in Amemiya et al. (2012). For each voxel, the normalized root-mean-square (RMS) between its time course shifted at each Δt and the reference time course is calculated, with the reference time course derived by convolving the standard HRF with the box-car function corresponding to the experimental design. The Δt at which the normalized RMS reaches the minimum is deemed the temporal shift of the voxel's time course relative to the reference.

2.5. Statistical analysis

2.5.1. Behavioral testing

Tactile detection threshold was calculated as the mean filament intensity across all reversal points in the staircase procedure.

Tactile localization error was calculated as the average straight-line

distance (in mm) between the perceived location and actual stimulus location. For each patient, localization performance on the contralateral hand was evaluated with the ipsilesional hand as a control. For this purpose, we randomly shuffled the relationship between trial-wise localization judgments and hand labels 100,000 times. The two-tailed permutation p-value was calculated as the percentage of permutations in which the absolute mean difference in localization error was larger than the actual absolute difference between the two hands. Permutation analyses were performed using DAAG package implemented in R (v4.1.1).

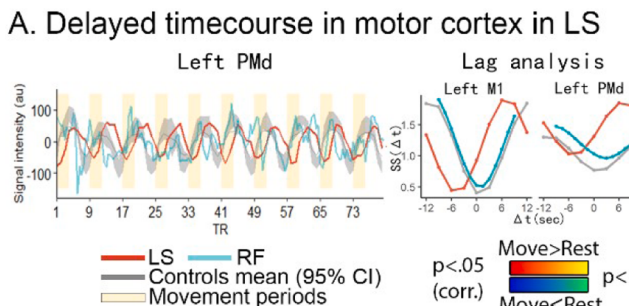
Proprioceptive localization error was calculated as the straight-line distance (in mm) between the perceived and actual hand location and permutation tests were performed between the two hands in the same manner as the tactile localization task.

2.5.2. Motor fMRI

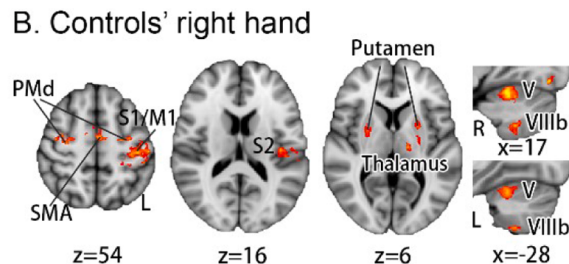
Functional neuroimaging data were analyzed using a univariate general linear model (GLM). The blood-oxygen-level-dependent (BOLD) signal for each run was modeled with 16 regressors. The experiment regressor was created by convolving the box-car function modelling movement phases with a standard double-gamma HRF. This regressor

implies the contrast of movement versus rest and its significance denotes motor activation level. The temporal derivative of the experiment regressor was added as a covariate of no interest to account for temporal variation in BOLD signal. An additional 14 nuisance regressors included six head motion parameters and their first derivative, mean time course from CSF, and mean time course from white-matter. Within each individual, runs of each hand were combined using a fixed-effects analysis. Group-analysis of controls was performed with a mixed-effects analysis using the FLAME 1 method in FSL. Results were thresholded at $p < .001$ and cluster-wise corrected at $p < .05$ based on Gaussian Random Field (GRF) theory (Worsley, 2001). Regions were identified based on atlases provided in FSL (Harvard-Oxford Cortical Structural Atlas, Juelich Histological Atlas, and Talairach Daemon Labels) and the Brodmann Area template provided in MRIcron.

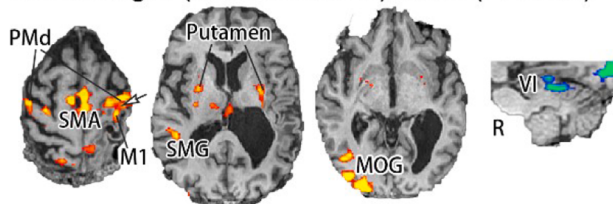
FLOBS analysis: As it is unlikely that hemodynamic lag in perilesional regions would affect subcortical or cerebellar areas, we modelled BOLD signal using the standard HRF in these regions in LS. However, as shown by the whole-brain lag analysis, LS's BOLD response to hand movement varied across brain regions (Figure S3), ranging from no temporal shift (in putamen) to lagging by nearly six seconds or more (e.g., motor cortex). The six-second lag had a dramatic impact such that no



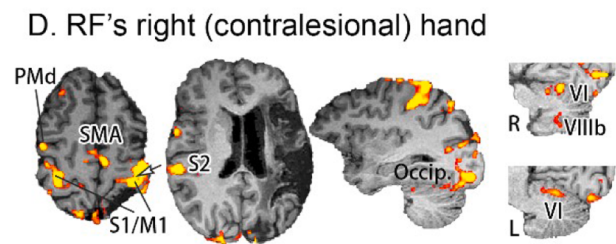
A. Delayed timecourse in motor cortex in LS



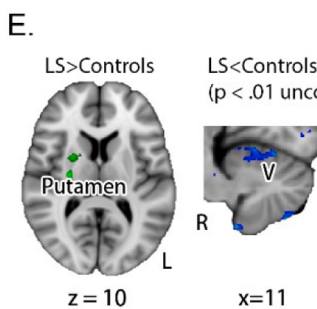
B. Controls' right hand



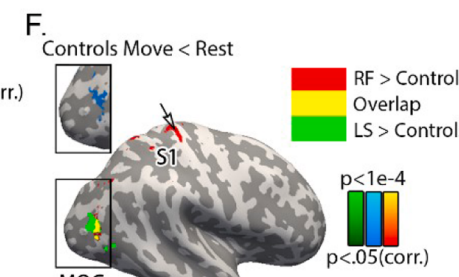
C. LS's right (contralesional) hand (FLOBS)



D. RF's right (contralesional) hand



E. LS > Controls



F. LS < Controls ($p < .01$ uncorr.)

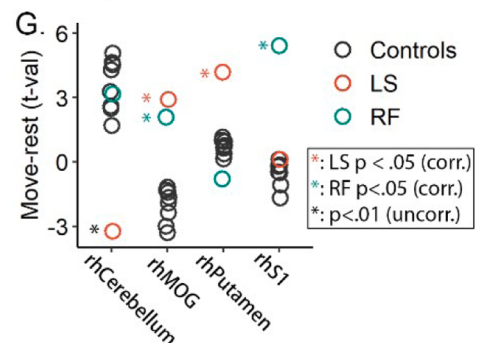


Fig. 2. Brain activation when participants moved their right hand. A. Average (demeaned) time-course of the right-hand motor runs shows that LS's hemodynamic response lags behind controls' and RF's in PMd. Lag analysis revealed a delay of 6 s in LS's hemodynamic response in M1 and PMd, as shown by the left-shifted red curves. B. In controls, moving the right hand significantly activated left primary somatosensory and motor cortex (SMC), bilateral PMd and SMA, bilateral putamen and cerebellum, left thalamus and S2. C. Regions with significant activity for right hand movement for LS (FLOBS analysis). While showing significant activity in left M1, bilateral PMd, SMA, and putamen as with controls, LS showed significant activation in right MOG and deactivation in right cerebellum (standard analysis). D. Regions with significant activity for right hand movement in RF. Other than left SMC, bilateral PMd and SMA, and cerebellum, RF showed significant activity in right S1 and M1, and right occipital lobe. Notably, the spared strip in S1 hand area was also activated. E-F. Whole-brain Crawford-Howell t -test. Based on the standard analysis, LS showed stronger activation in right putamen compared with controls. The right cerebellum was less activated than controls (ROI level $p < .01$ uncorrected). Both LS and RF showed significantly stronger activation in right MOG, an area that was significantly deactivated during movement in controls. RF also showed stronger activation in right S1. G. T-values in ROIs sampled based on E. and F. Asterisks reflect significance level from the whole-brain analysis. PMd: Dorsal premotor cortex. PMv: Ventral premotor cortex. SMA: Supplementary motor area. SMG: Supramarginal gyrus. MOG: Middle occipital gyrus. Occip.: Occipital lobe.

activation in motor cortex was found when modeled with the standard HRF (**Figure S4A**), yet there was a clear motor-evoked BOLD response (**Fig. 2A**, **Figure S4B**). To account for the delay, we additionally analyzed LS's motor data in cortical regions using the FLOBS (FMRIB's Linear Optimal Basis Sets) toolkit in FSL (West et al., 2019). This method allowed us to specify the range of parameters that determine the shape of the HRF. A set of basis functions was then generated whose weighted combinations span possible HRFs that satisfy the specified parameters. We set the initial delay of the HRF to range from 0 to 6 s to account for the delay in LS's BOLD signal and selected the first six basis functions that collectively explain >95% of the variance of the sample HRFs. Each run of LS's data was modeled with these six basis functions along with nuisance regressors. Significance of the first basis function regressor, which has the shape of a canonical HRF and implies motor activity versus rest, denotes motor activation level. To assess model performance, we sampled key regions of interest and calculated percentage variance explained (R-square) of the experiment regressor and of the full model of the FLOBS analysis and compared with the standard analysis. This assessment verified improved model fit by FLOBS compared with the standard analysis in LS's motor cortex that was specifically contributed by the experiment regressor (**Figure S4B**). No temporal delay was observed in RF (**Figure S3**).

To directly compare each brain-damaged individual with controls, we performed voxel-wise Crawford-Howell *t*-tests for each hand separately (Crawford and Howell, 1998) on the *t*-value of the movement-versus-rest contrast between each patient and controls across the whole brain, masking out the lesioned areas of each patient. For LS, this analysis was performed twice, once with results from the standard analysis and once with the FLOBS analysis for reasons discussed above. Results are thresholded at $p < .01$ and cluster-wise corrected at $p < .05$ based on GRF theory. Individual *t*-values were extracted from the resulting regions and plotted to visualize the distribution. When noted, Crawford-Howell *t*-tests were performed on the mean *t*-value across voxels within an ROI to explore effects at the ROI level that may not survive whole-brain multiple comparisons correction.

2.5.3. Visual control fMRI

Data were analyzed using the same pipeline as in the motor experiment. The contrast of word versus fixation cross was computed within each control participant and one-sample *t*-tests were performed on the *t*-values within ROIs where LS and RF showed different levels of activation compared with controls.

2.5.4. Somatosensory fMRI

Data were analyzed using the same pipeline as with the motor experiment, except the experiment regressor was generated based on the design of the somatosensory experiment. The experiment regressor implies the contrast of stimulation versus rest and its significance denotes somatosensory activation level. Results were thresholded at $p < .001$ voxel-wise and cluster-wise corrected at $p < .05$ based on GRF theory.

3. Results

3.1. Impaired tactile abilities in LS and RF

Both LS and RF showed elevated detection thresholds on the contralateral right hand (4 g and 8 g respectively), demonstrating diminished protective sensation. The ipsilesional left hand showed normal detection thresholds (0.07 g for LS, 0.6 g for RF; Hage et al., 1998). In addition, both individuals made significantly larger tactile localization errors on the contralateral hand (LS: $M = 51.5$ mm, $SD = 29.0$ mm; RF: $M = 55.5$ mm, $SD = 32.6$ mm) compared with the ipsilesional hand (LS: $M = 10.5$ mm, $SD = 10.1$ mm; RF: $M = 5.3$ mm, $SD = 7.1$ mm; permutation $p < 0.001$; **Figure S2A**). LS demonstrated an impaired ability in localizing the contralateral hand without vision (Contralateral hand: *localization judgment error* = 93.5 mm, $SD = 41.8$ mm, Ipsilesional

hand: $M = 56.2$ mm, $SD = 42.6$ mm, permutation $p < .001$; see **Figure S2B**). These findings suggest that the motor deficits on the contralateral hand of LS and RF when vision was not available likely stem from degraded somatosensory feedback. We then examined how the motor network in the brain responds to hand movement when somatosensory inputs are compromised due to S1 damage.

3.2. Contralateral motor activation

We first analyzed activation induced by movement of the right (contralateral) hand in the brain-damaged individuals and controls. In controls, movement of the right hand activated cortical sensorimotor areas including contralateral left primary somatosensory and motor cortex (SMC), left S2, bilateral dorsal premotor cortex (PMd) and supplementary motor area (SMA; **Fig. 2B**). Subcortical activation was found in left thalamus, bilateral putamen, and bilateral anterior (lobule V) and posterior (lobule VIIIb) cerebellum.

In LS, the same cortical motor areas – left M1, bilateral PMd and SMA – were activated as in controls (**Fig. 2C**). No activation was seen in left S1 and S2 due to the lesion. As with controls, bilateral putamen was activated. Thalamic activation was also found, albeit on the right side ipsilateral to the moving hand. In addition, right supramarginal gyrus (SMG) and middle occipital gyrus (MOG) responded to hand movement, patterns not observed in controls. Finally, whereas the FLOBS analysis did not reveal activation in cerebellum, the standard analysis (with standard HRF) showed deactivation in lobule V in right cerebellum (see **Figure S5A** for the time course and lag analysis in this region). Whole-brain Crawford-Howell *t*-test between LS and controls revealed greater activity in right MOG (**Fig. 2F**) and right putamen (**Fig. 2E**). The cerebellar deactivation in LS manifested as significantly lower activity relative to controls ($p = .001$ at ROI level, **Fig. 2E**). The activity in MOG in LS is unlikely driven by visual stimuli (i.e. word instructions vs. fixation cross) because controls showed less activity in this area during hand movement (**Fig. 2F** and **2G**) and the same trend of deactivation was seen during word presentation alone in the visual control experiment ($t(6) = -2.42$, $p = .052$).

In RF, moving the contralateral hand resulted in significant activity in bilateral PMd, SMA, as well as bilateral anterior cerebellum, as with controls (**Fig. 2D**). There were three findings of note for RF. First, the spared contralateral S1, along with M1, was activated, consistent with controls. Second, ipsilateral (to the moving hand) primary sensorimotor cortex was also activated, whereas controls only showed contralateral activation. Finally, significant activity was found in right occipital lobe including MOG. In contrast to LS and controls, no significant activity was seen in bilateral putamen. Ipsilateral right S2, as opposed to left S2 in controls, was activated, therefore both S1 and S2 demonstrated ipsilateral activation. Whole-brain Crawford-Howell *t*-test between RF and controls revealed greater activation in right MOG, overlapping with where LS had stronger activity, and in right S1 ipsilateral to the moving hand (**Fig. 2F**). The activation in MOG is located at the parietal-occipital sulcus and extends into Brodmann area (BA) 19 and BA37, close to and dorsal-posterior to the extrastriate body area (EBA, **Figure S6**; Downing et al., 2001; Peelen and Downing, 2005).

To summarize, while both LS and RF showed greater activation in right MOG relative to controls, LS demonstrated subcortical changes with higher activation in putamen and reduced activity in cerebellum, whereas RF presented cross-hemispheric changes with increased activity in contralateral S1 ipsilateral to the moving right hand.

Notably, the spared portion of left S1 in RF was activated by hand movement, potentially indicating preserved somatosensory functions in this area. On the other hand, the substantially impaired tactile and proprioceptive abilities in RF are somewhat inconsistent with the function of the spared left S1. Alternatively, the activation in S1 could be a spread of M1 activation due to spatial smoothing. To tease apart these possibilities, and to address the general question of how S1 damage influences the rest of the somatosensory network, we conducted a

somatosensory fMRI experiment on LS and RF, with the ipsilesional hand serving as a within-subjects control.

3.3. Somatosensory activation

Despite substantial damage in S1, both individuals reported feeling touch during the experiment. In RF, the spared portion of left S1 was also activated by tactile stimulation on the contralateral right hand (Fig. 3A), overlapping with motor activation, suggesting residual somatosensory function in this area. In addition, several ipsilateral (right) areas including PMd, PMv, and IPS responded to tactile stimulation, showing shared activation with the left hand activation (Fig. 3B). This pattern is consistent with motor activation in that the somatosensory activation shifted to the intact hemisphere. Tactile stimulation on the left hand activated a wide sensorimotor network including right SMC, right premotor and parietal cortex, bilateral LOTC, and bilateral cerebellum (Fig. 3B).

In LS, no activation in left S1 was seen due to the lesion. Nevertheless, tactile stimulation on the contralateral right hand activated association areas including left S2, left PMd, left SMA, left frontal operculum, right superior temporal sulcus, and right cerebellum (Fig. 3C), suggesting alternative pathways to S1. These areas are homotopic to areas activated by tactile stimulation on the ipsilesional left hand (Fig. 3D). Overlapping the cerebellar area that was deactivated when LS moved his right hand (Fig. 2C), we found activation elicited by somatosensory stimulation of the left hand and no hemodynamic response lag (Figure S3, Figure S5B), suggesting that the motor deactivation in this area is unlikely driven by altered blood flow perfusion.

3.4. Ipsilesional hand movement

Finally, we present results when participants moved their left (ipsilesional) hand. In controls, moving the left hand activated right SMC, right PMd, bilateral SMA, and left S2 (Fig. 4A). Subcortical activation

was observed in right thalamus and bilateral cerebellum (Fig. 4A). The same cortical sensorimotor areas, namely right SMC, right PMd, and SMA, along with left cerebellum were also activated in LS (Fig. 4B). LS also showed activation in ipsilateral left M1 and PMd, bilateral putamen, and bilateral MOG (Fig. 4B). RF, with typical activation in right S1/M1, right PMd, and SMA, also demonstrated significant activation in bilateral occipital lobes that was not observed in controls (Fig. 4C).

Crawford-Howell *t*-tests revealed similar patterns as observed for moving the contralateral right hand. Specifically, we found stronger activation in right S1 in RF (Fig. 4D) and in bilateral putamen in LS (Fig. 4D) compared with controls. LS also showed increased activation in right S1 compared with controls at ROI level ($p = .003$). Right MOG was more strongly activated in RF from the whole-brain analysis (Fig. 4D), as well as in LS based on an ROI Crawford-Howell *t*-test (ROI-level $p = .007$, Fig. 4D, point graph).

4. Discussion

We examined two brain-damaged individuals to study the reorganization of somatosensory and motor functions after damage to S1. First, when moving their contralateral right hand, RF (small island of remaining S1) showed greater activation in ipsilateral right S1 compared with controls, while LS (no remaining S1 hand area) showed greater activation in right putamen and surprisingly, less activation in right cerebellum. Second, both LS and RF showed greater activity in right MOG during movement compared to controls. Third, tactile stimulation of the contralateral hand activated spared S1 in RF, whereas in LS activation was seen in higher-order sensory and motor areas.

4.1. Cerebellar deactivation and increased activity in putamen in LS

Comparing LS with age-matched controls, we found greater activation in right putamen and less activation in right sensorimotor cerebellum, which was deactivated in LS during movement versus rest.

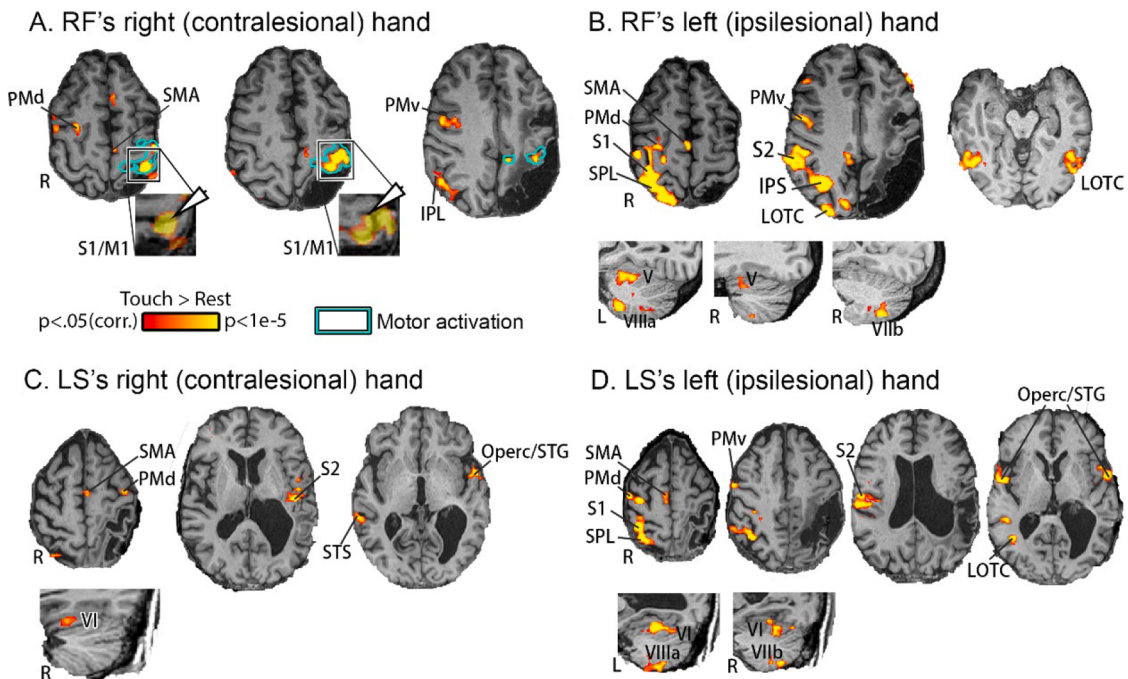


Fig. 3. Somatosensory activation in RF and LS. A. Somatosensory stimulation on RF's contralateral right hand activated the spared portion of left S1, overlapping with the motor activation. B. Tactile stimulation on RF's left hand activated right S1, S2, PMd, PMv, SMA, SPL, IPS, and bilateral LOTC. C. Despite near-complete damage in S1, somatosensory stimulation on LS's contralateral right hand activated higher-level sensorimotor areas including left SMA, PMd, S2, STG/frontal operculum, right STS and cerebellum. D. Similar to RF's ipsilesional hand, tactile stimulation on LS's left hand activated right S1, S2, PMd, PMv, SMA, SPL, bilateral STG/frontal operculum and cerebellum. SPL: Superior parietal lobule. IPS: Intraparietal sulcus. Operc: Operculum. STG: Superior temporal gyrus. STS: Superior temporal sulcus. LOTC: Lateral occipital-temporal cortex.

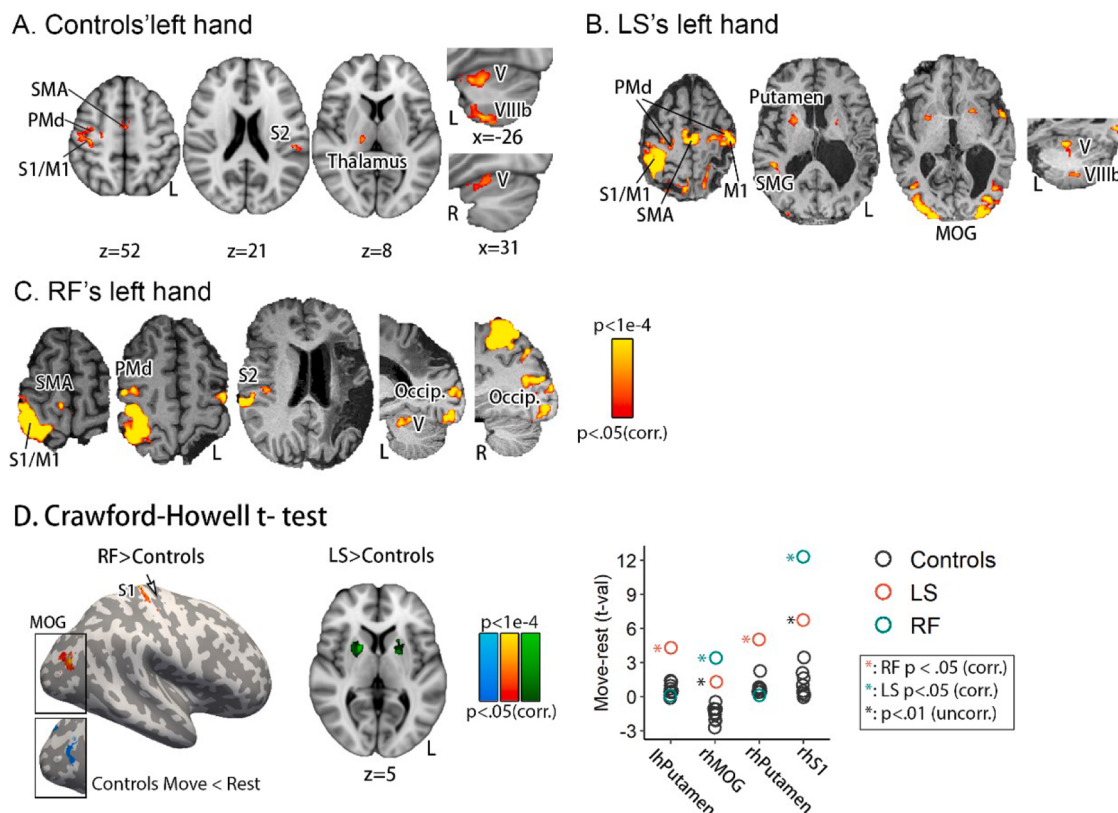


Fig. 4. Brain activation when participants moved the left hand. A. In controls, moving the left hand activated right SMC, SMA, PMd, thalamus, left PMv, S2, and bilateral cerebellum. B. In LS, moving the left hand activated a similar motor network and additionally left and right MOG. C. In RF, moving the right hand activated typical motor networks and additionally right occipital lobe. D. Whole-brain Crawford-Howell *t*-tests revealed significantly greater activity in right MOG (where controls showed a significant deactivation) and S1 in RF relative to controls, and in bilateral putamen in LS relative to controls. ROI *t*-tests showed significantly stronger activity in LOTC also in LS relative to controls.

In right cerebellum, while controls showed significant activation during movement (lobules V-VI), LS demonstrated the opposite pattern – less activation during movement versus rest. During movement execution, the motor system predicts the sensory consequence of a motor command in compensation for delayed sensory feedback (Wolpert et al., 1995), a process proposed to be performed by the cerebellum (Blakemore et al., 2001; Izawa et al., 2012; Nowak et al., 2007; Shadmehr and Krakauer, 2008; Wong et al., 2019). The sensory prediction function involves both cerebellum and S1, regions that project to (Glickstein, 1997; Sultan et al., 2012) and modulate (Gold and Lauritzen, 2002; Kilteni and Ehrsson, 2020; Matsui et al., 2012; Restuccia et al., 2001) each other. Moreover, an absence of sensory input (due to neuropathies) but with intact S1 does not necessarily eliminate motor activity in cerebellum, suggesting the importance of S1 integrity in maintaining cerebellar activation (Weeks et al., 1999). In LS, we propose that deactivation of cerebellum during movement reflects inhibition of the sensory prediction function due to absence of sensory feedback and reduced input from S1.

An alternative interpretation is that the cerebellar findings in LS are due to hemodynamic lags caused by stroke (Amemiya et al., 2012; Bonakdarpour et al., 2007). We consider these results to more likely reflect deactivation for two reasons. First, hemodynamic lag is known to occur in perilesional but not remote areas. One study examined blood flow in patients with ischemia or hypoperfusion and found a delayed hemodynamic response in bilateral motor cortex but *not* in cerebellum (Amemiya et al., 2012). Second, the same area showed activation in the somatosensory experiment with minimal HRF lag (see Figure S3, Figure S5B). This suggests that our results are due to an actual change in cerebellar function in the face of somatosensory damage. Our results suggest a re-weighting of the motor system in compensation for absence

of S1, wherein the relative weight was increased for the loop responsible for motor output (i.e., putamen), and decreased for the loop responsible for sensory processing (i.e., cerebellum).

The basal ganglia are active during action selection and decision-making, whereas cerebellum is responsible for estimating and processing the sensory consequences of movement (Doya, 2000; Jueptner and Weiller, 1998; Shadmehr and Krakauer, 2008). For example, the putamen is more strongly activated when performing self-timed versus externally-cued movements in non-human primates (Lee et al., 2006) and this activity is dramatically reduced for passive compared to active movements (Jueptner and Weiller, 1998; Liles 1985). Furthermore, patients with Parkinson's disease, associated with basal ganglia degeneration, show substantial difficulty in performing voluntary actions versus visually-guided action (Jackson et al., 1995; see also Mizes et al., 2023a). The increased putaminal activity in LS may reflect increased effort in selecting the correct motor plan (i.e., open or close the hand) under diminished somatosensory feedback.

4.2. Increased activity in right S1 in RF

In RF, movement of the contralateral right hand activated typical motor networks. In addition, ipsilateral (to the moving hand) S1 was more strongly activated compared to controls, demonstrating reorganization to the contralateral hemisphere. Interestingly, such bilateral S1 activation was not observed in the somatosensory fMRI experiment (Fig. 3), suggesting that it is specific to motor function. There is abundant evidence for the involvement of contralateral motor cortex when individuals with brain damage move the contralateral hand (Carey et al., 2006; Favre et al., 2014; Grefkes and Ward, 2014; Rehme et al., 2012; Ward et al., 2003), yet the involvement of contralateral

somatosensory cortex remains unexplored. To our knowledge, this is the first report of contralateral somatosensory activity subsequent to S1 lesion. Increased activation in the contralesional hemisphere may result from decreased inhibition by the lesioned hemisphere or increased reliance on ipsilateral (to the moving hand) sensorimotor pathways (Grefkes and Ward, 2014; Medina and Rapp, 2008).

Why did LS and RF show substantially different activation patterns despite lesioned S1 and spared M1 in both cases? We speculate that these distinct reorganization patterns could be driven by different extents of their S1 lesions. Whereas LS suffered a complete lesion of the hand area in S1 and accordingly demonstrated no S1 activation for contralesional hand tactile stimulation, RF had a spared strip of S1 along the anterior bank that responded to touch. The spared tissue may represent residual tactile information from the hand, maintaining the connections between S1 and M1, basal ganglia, and cerebellum, thus preserving a typical motor network. Moreover, the spared S1 may have driven cross-hemispheric somatosensory reorganization via transcallosal connections (Grefkes and Ward, 2014). Animal studies found increased reorganization in remote areas (e.g., bilateral premotor cortex) with larger M1 lesions (Dancause et al., 2006; Dijkhuizen et al., 2003; Frost et al., 2003; Touvkyne et al., 2016), and more substantial reorganization within S1 with more complete dorsal column lesions (Qi et al., 2019). We report for the first time from human subjects the effect of the extent of lesion size in the hand area in S1 on motor network organization. We note that the lesion extent also differs in other brain regions between LS and RF, with more severe damage in posterior parietal cortex (PPC) and inferior frontal gyrus (IFG) in RF compared to LS. While we cannot directly attribute the different motor activation patterns to specific lesions, the better manual abilities in RF, despite more severe lesions in PPC and IFG, indicates that the spared tissue in S1 might play a key role in the preservation of motor functions in RF.

4.3. Increased MOG activity in both LS and RF

In both RF and LS, contralesional hand movement elicited activation in right MOG that was, surprisingly, significantly deactivated in controls. The MOG cluster is located dorsal-posterior to the extrastriate body area (EBA), a region that responds to images of body parts versus other object categories (Figure S6; Downing et al., 2001; 2006; Pilgramm et al., 2016; Weiner and Grill-Spector, 2011). Although reported to be activated by the execution of hand and tool-use actions (Brandi et al., 2014; Gallivan et al., 2011; also see Hinkley et al., 2011), few studies have specified the function of MOG in motor control. We present two possible hypotheses for why it may be active in RF and LS. First, MOG has been associated with processing feedback (Bermann et al., 2012) and when the consequences of an action were incongruent with the participant's intention (Yomogida et al., 2010). One possibility is that LS and RF relied more on active feedback monitoring relative to controls, thus activating MOG. Second, MOG has been associated with processing body stimuli, including viewing other people making gestures (Husain et al., 2009), inferring others' action intention in a visual scene (Atique et al., 2011), and mental rotation of hand stimuli (Vingerhoets et al., 2002). A second possible explanation is that LS and RF adopt visual motor imagery in absence of sensory feedback (Čeko et al., 2013; Ter Horst et al., 2012; Mercier et al., 2008), leading to stronger MOG activity. We note that the underlying mechanism of MOG involvement in motor control requires more experiments, yet our findings provide the first evidence that visual cortex compensates for sensory loss in motor control.

4.4. Neural correlates of tactile perception after S1 damage

In LS, tactile stimulation on the contralesional right hand activated left S2 and frontal motor areas in absence of S1 activation. RF, however, showed activation in spared left S1 as well as right association areas. Both individuals reported feeling the touch during the experiment.

Studies on both humans and non-human primates found that activity in higher-level areas such as SMA, PMd, and S2, but not in S1, coincides with conscious tactile detection (Grund et al., 2021; Hernández et al., 2002; Lafuente and Romo, 2005; Moore et al., 2013; Tamè and Holmes, 2016). Along this line, sensory association areas may receive tactile inputs from different routes in LS and RF, giving rise to their tactile perception via different mechanisms. In LS, S2 may receive information from thalamic projections and then send this tactile signal to frontal motor areas (Friedman and Murray, 1986; Garraghty et al., 1991; Hernández et al., 2002; Rowe et al., 1996). In RF, the preserved S1 receives thalamic projections and feeds forward to higher-level areas. In either case, tactile detection is supported by existing neural substrates, but these substrates are insufficient to support accurate tactile localization.

4.5. Study limitations

First, our study has a small sample size of two brain damaged individuals. While the rarity of the lesion pattern makes it difficult to amass a large sample size, future research is needed to accumulate evidence regarding motor reorganization after S1 damage. Second, our interpretations of MOG activity in LS and RF are speculative and would require additional experiments to test, for example, the visual control experiment performed only in controls and a potential motor imagery experiment to examine the role of MOG in imagery. Future studies may directly test these hypotheses with more cases or controlled lesioning methods in animal models.

In summary, we examined motor reorganization in two rare cases with substantially damaged S1 but primarily intact M1. LS, with a more profound lesion in S1 hand area, showed increased putaminal activation and cerebellar deactivation when moving the contralesional hand, suggesting re-balancing between motor output and sensory processing within motor networks. RF, with a strip of S1 hand area spared, demonstrated cross-hemispheric S1 reorganization. Both individuals showed increased activity in right MOG compared to controls, indicating compensatory visual imagery processes. These findings provide novel evidence for long-range motor reorganization and visual recruitment subsequent to S1 damage in human subjects, adding knowledge regarding the differential roles across motor regions in sensorimotor integration.

CRediT authorship contribution statement

Yuqi Liu: Writing – review & editing, Writing – original draft, Visualization, Methodology, Investigation, Formal analysis, Data curation, Conceptualization. **Elizabeth J. Halfen:** Investigation. **Jeffrey M. Yau:** Writing – review & editing, Supervision, Investigation. **Simon Fischer-Baum:** Writing – review & editing, Supervision, Investigation. **Peter J. Kohler:** Methodology. **Olufunsho Faseyitan:** Investigation, Data curation. **H. Branch Coslett:** Supervision, Project administration, Conceptualization. **Jared Medina:** Writing – review & editing, Supervision, Project administration, Funding acquisition, Data curation, Conceptualization.

Declaration of competing interest

The authors declare no conflicts of interest.

Acknowledgements

We are grateful to LS and RF and all control participants for their dedication to this project. We would like to thank Emily Baumert, Michael Grzenda, Alexandria O'Neal, and Charlotte Wilkinson for their work on this project. This work was supported by grants from the National Natural Science Foundation of China (32200843 to Y.L.) and the National Science Foundation (1632849 to J.M.). This work is partially

based upon work conducted by S. F-B. supported by the Independent/Research Development program while serving at the National Science Foundation.

Supplementary materials

Supplementary material associated with this article can be found, in the online version, at doi:10.1016/j.neuroimage.2025.121336.

Data availability

Source data from behavioral tasks can be found at <https://osf.io/zh6hb/>. As our participants are brain-damaged individuals whose brain images are identifiable, we are not sharing our neuroimaging data to public.

References

- Amemiya, S., Kunitatsu, A., Saito, N., Ohtomo, K., 2012. Impaired hemodynamic response in the ischemic brain assessed with BOLD fMRI. *Neuroimage* 61 (3), 579–590.
- Atique, B., Erb, M., Gharabagi, A., Grodd, W., Anders, S., 2011. Task-specific activity and connectivity within the mentalizing network during emotion and intention mentalizing. *Neuroimage* 55 (4), 1899–1911.
- Berman, B.D., Horowitz, S.G., Venkataraman, G., Hallett, M., 2012. Self-modulation of primary motor cortex activity with motor and motor imagery tasks using real-time fMRI-based neurofeedback. *Neuroimage* 59 (2), 917–925.
- Blakemore, S.-J., Frith, C.D., Wolpert, D.M., 2001. The cerebellum is involved in predicting the sensory consequences of action. *Neuroreport* 12 (9), 1879–1884.
- Bonakdarpour, B., Parrish, T.B., Thompson, C.K., 2007. Hemodynamic response function in patients with stroke-induced aphasia: implications for fMRI data analysis. *Neuroimage* 36 (2), 322–331.
- Brandi, M.L., Wohlschläger, A., Sorg, C., Hermsdörfer, J., 2014. The neural correlates of planning and executing actual tool use. *J. Neurosci.* 34 (39), 13183–13194.
- Carey, L.M., Abbott, D.F., Egan, G.F., O'Keefe, G.J., Jackson, G.D., Bernhardt, J., Donnan, G.A., 2006. Evolution of brain activation with good and poor motor recovery after stroke. *Neurorehabil. Neural Repair.* 20 (1), 24–41.
- Carey, J.R., Kimberley, T.J., Lewis, S.M., Auerbach, E.J., Dorsey, L., Rundquist, P., Ugurbil, K., 2002. Analysis of fMRI and finger tracking training in subjects with chronic stroke. *Brain* 125 (4), 773–788.
- Carey, L.M., Matyas, T.A., Baum, C., 2018. Effects of somatosensory impairment on participation after stroke. *Am. J. Occup. Ther.* 72 (3), 7203205100p1–7203205100p10.
- Catani, M., Dell'Acqua, F., Vergani, F., Malik, F., Hodge, H., Roy, P., De Schotten, M.T., 2012. Short frontal lobe connections of the human brain. *Cortex* 48 (2), 273–291.
- Ceko, M., Seminowicz, D.A., Bushnell, M.C., Olausson, H.W., 2013. Anatomical and functional enhancements of the insula after loss of large primary somatosensory fibers. *Cereb. Cortex* 23, 2017–2024.
- Chen, P.L., Hsu, H.Y., Wang, P.Y., 2006. Isolated hand weakness in cortical infarctions. *J. Formos. Med. Assoc.* 105 (10), 861–865.
- Crawford, J.R., Howell, D.C., 1998. Comparing an individual's test score against norms derived from small samples. *Clin. Neuropsychol.* 12 (4), 482–486.
- Dancause, N., Barbay, S., Frost, S.B., Zoubina, E.V., Plautz, E.J., Mahnken, J.D., Nudo, R.J., 2006. Effects of small ischemic lesions in the primary motor cortex on neurophysiological organization in ventral premotor cortex. *J. Neurophysiol.* 96 (6), 3506–3511.
- de Lafuente, V., Romo, R., 2005. Neuronal correlates of subjective sensory experience. *Nat. Neurosci.* 8 (12), 1698–1703.
- Dijkhuizen, R.M., Singhal, A.B., Mandeville, J.B., Wu, O., Halpern, E.F., Finklestein, S.P., Lo, E.H., 2003. Correlation between brain reorganization, ischemic damage, and neurologic status after transient focal cerebral ischemia in rats: a functional magnetic resonance imaging study. *J. Neurosci.* 23 (2), 510–517.
- Downing, P.E., Jiang, Y., Shuman, M., Kanwisher, N., 2001. A cortical area selective for visual processing of the human body. *Science* 293 (5539), 2470–2473.
- Downing, P.E., Peelen, M.V., Wiggett, A.J., Tew, B.D., 2006. The role of the extrastriate body area in action perception. *Soc. Neurosci.* 1 (1), 52–62.
- Doya, K., 2000. Complementary roles of basal ganglia and cerebellum in learning and motor control. *Curr. Opin. Neurobiol.* 10 (6), 732–739.
- Eickhoff, S.B., Laird, A.R., Grefkes, C., Wang, L.E., Zilles, K., Fox, P.T., 2009. Coordinate-based activation likelihood estimation meta-analysis of neuroimaging data: a random-effects approach based on empirical estimates of spatial uncertainty. *Hum. Brain Mapp.* 30 (9), 2907–2926.
- Favre, I., Zeffiro, T.A., Detante, O., Krainik, A., Hommel, M., Jaillard, A., 2014. Upper limb recovery after stroke is associated with ipsilesional primary motor cortical activity: a meta-analysis. *Stroke* 45 (4), 1077–1083.
- Friedman, D.P., Murray, E.A., 1986. Thalamic connectivity of the second somatosensory area and neighboring somatosensory fields of the lateral sulcus of the macaque. *J. Comp. Neurol.* 252 (3), 348–373.
- Frost, S.B., Barbay, S., Friel, K.M., Plautz, E.J., Nudo, R.J., 2003. Reorganization of remote cortical regions after ischemic brain injury: a potential substrate for stroke recovery. *J. Neurophysiol.* 89 (6), 3205–3214.
- Gallivan, J.P., McLean, D.A., Smith, F.W., Culham, J.C., 2011. Decoding effector-dependent and effector-independent movement intentions from human parieto-frontal brain activity. *J. Neurosci.* 31 (47), 17149–17168.
- Garraghty, P.E., Florence, S.L., Tenhula, W.N., Kaas, J.H., 1991. Parallel thalamic activation of the first and second somatosensory areas in prosimian primates and tree shrews. *J. Comp. Neurol.* 311 (2), 289–299.
- Ghosh, S., Porter, R., 1988. Corticocortical synaptic influences on morphologically identified pyramidal neurones in the motor cortex of the monkey. *J. Physiol. (L.)* 400 (1), 617–629.
- Glickstein, M., 1997. Mossy-fibre sensory input to the cerebellum. *Prog. Brain Res.* 114, 251–259.
- Gold, L., Lauritzen, M., 2002. Neuronal deactivation explains decreased cerebellar blood flow in response to focal cerebral ischemia or suppressed neocortical function. *Proc. Natl. Acad. Sci.* 99 (11), 7699–7704.
- Grefkes, C., Fink, G.R., 2011. Reorganization of cerebral networks after stroke: new insights from neuroimaging with connectivity approaches. *Brain* 134 (5), 1264–1276.
- Grefkes, C., Nowak, D.A., Eickhoff, S.B., Dafotakis, M., Küst, J., Karbe, H., Fink, G.R., 2008. Cortical connectivity after subcortical stroke assessed with functional magnetic resonance imaging. *Ann. Neurol.* 63 (2), 236–246.
- Grefkes, C., Ward, N.S., 2014. Cortical reorganization after stroke: how much and how functional? *Neuroscientist* 20 (1), 56–70.
- Grund, M., Forschack, N., Nierhaus, T., Villringer, A., 2021. Neural correlates of conscious tactile perception: an analysis of BOLD activation patterns and graph metrics. *Neuroimage* 224, 117384.
- Hage, J.J., Ahmed, A.K.J., de Groot, P.J., De Boer, E., 1998. Differential of sensibility of the hand using Semmes-Weinstein monofilaments. *Hand. Surg.* 3 (02), 237–245.
- Hardwick, R.M., Caspers, S., Eickhoff, S.B., Swinnen, S.P., 2018. Neural correlates of action: comparing meta-analyses of imagery, observation, and execution. *Neurosci. Biobehav. Rev.* 94, 31–44.
- Harrison, T.C., Silasi, G., Boyd, J.D., Murphy, T.H., 2013. Displacement of sensory maps and disorganization of motor cortex after targeted stroke in mice. *Stroke* 44 (8), 2300–2306.
- Hernández, A., Zainos, A., Romo, R., 2002. Temporal evolution of a decision-making process in medial premotor cortex. *Neuron* 33 (6), 959–972.
- Hinkley, L.B., Nagarajan, S.S., Dalal, S.S., Guggisberg, A.G., Disbrow, E.A., 2011. Cortical temporal dynamics of visually guided behavior. *Cereb. Cortex* 21 (3), 519–529.
- Husain, F.T., Patkin, D.J., Thai-Van, H., Braun, A.R., Horwitz, B., 2009. Distinguishing the processing of gestures from signs in deaf individuals: an fMRI study. *Brain Res.* 1276, 140–150.
- Izawa, J., Criscimagna-Hemminger, S.E., Shadmehr, R., 2012. Cerebellar contributions to reach adaptation and learning sensory consequences of action. *J. Neurosci.* 32 (12), 4230–4239.
- Jaillard, A., Martin, C.D., Garambois, K., Lebas, J.F., Hommel, M., 2005. Vicarious function within the human primary motor cortex? A longitudinal fMRI stroke study. *Brain* 128 (5), 1122–1138.
- Jackson, S.R., Jackson, G.M., Harrison, J., Henderson, L., Kennard, C., 1995. The internal control of action and Parkinson's disease: a kinematic analysis of visually-guided and memory-guided prehension movements. *Exp. Brain Res.* 105, 147–162.
- Jeannerod, M., Michel, F., Prablanc, C., 1984. The control of hand movements in a case of hemianesthesia following a parietal lesion. *Brain* 107 (3), 899–920.
- Jenkinson, E.W., Glickstein, M., 2000. Whiskers, barrels, and cortical efferent pathways in gap crossing by rats. *J. Neurophysiol.* 84 (4), 1781–1789.
- Jueptner, J., Jueptner, M., Jenkins, I.H., Brooks, D.J., Frackowiak, R.S.J., Passingham, R.E., 1996. The sensory guidance of movement: a comparison of the cerebellum and basal ganglia. *Exp. Brain Res.* 112, 462–474.
- Jueptner, M., Weiller, C., 1998. A review of differences between basal ganglia and cerebellar control of movements as revealed by functional imaging studies. *Brain: J. Neurol.* 121 (8), 1437–1449.
- Kambi, N., Tandon, S., Mohammed, H., Lazar, L., Jain, N., 2011. Reorganization of the primary motor cortex of adult macaque monkeys after sensory loss resulting from partial spinal cord injuries. *J. Neurosci.* 31 (10), 3696–3707.
- Kato, H., Izumiya, M., 2015. Impaired motor control due to proprioceptive sensory loss in a patient with cerebral infarction localized to the postcentral gyrus. *J. Rehabil. Med.* 47 (2), 187–190.
- Kiltuni, K., Ehrsson, H.H., 2020. Functional connectivity between the cerebellum and somatosensory areas implements the attenuation of self-generated touch. *J. Neurosci.* 40 (4), 894–906.
- LaMotte, R.H., Mountcastle, V.B., 1979. Disorders in somesthesia following lesions of parietal lobe. *J. Neurophysiol.* 42 (2), 400–419.
- Lee, I.H., Seitz, A.R., Assad, J.A., 2006. Activity of tonically active neurons in the monkey putamen during initiation and withholding of movement. *J. Neurophysiol.* 95 (4), 2391–2403.
- Liles, S.L., 1985. Activity of neurons in putamen during active and passive movements of wrist. *J. Neurophysiol.* 53 (1), 217–236.
- Lutkenhoff, E.S., Rosenberg, M., Chiang, J., Zhang, K., Pickard, J.D., Owen, A.M., Monti, M.M., 2014. Optimized brain extraction for pathological brains (optiBET). *PLoS. One* 9 (12), e115551.
- Mao, T., Kusefoglu, D., Hooks, B.M., Huber, D., Petreanu, L., Svoboda, K., 2011. Long-range neuronal circuits underlying the interaction between sensory and motor cortex. *Neuron* 72 (1), 111–123.
- Mathis, M.W., Mathis, A., Uchida, N., 2017. Somatosensory cortex plays an essential role in forelimb motor adaptation in mice. *Neuron* 93 (6), 1493–1503.
- Matsui, T., Koyano, K.W., Tamura, K., Osada, T., Adachi, Y., Miyamoto, K., Miyashita, Y., 2012. fMRI activity in the macaque cerebellum evoked by intracortical

- microstimulation of the primary somatosensory cortex: evidence for polysynaptic propagation. *PLoS. One* 7 (10), e47515.
- Medina, J., Rapp, B., 2008. Phantom tactile sensations modulated by body position. *Curr. Biol.* 18 (24), 1937–1942.
- Mercier, C., Aballea, A., Vargas, C.D., Paillard, J., Sirigu, A., 2008. Vision without proprioception modulates cortico-spinal excitability during hand motor imagery. *Cereb. Cortex* 18 (2), 272–277.
- Mizes, K.G., Lindsey, J., Escola, G.S., Ölveczky, B.P., 2023a. Dissociating the contributions of sensorimotor striatum to automatic and visually guided motor sequences. *Nat. Neurosci.* 26 (10), 1791–1804.
- Mizes, K.G., Lindsey, J., Escola, G.S., & Ölveczky, B.P. (2023b). Motor cortex is required for flexible but not automatic motor sequences. *bioRxiv*.
- Moore, C.I., Crosier, E., Greve, D.N., Savoy, R., Merzenich, M.M., Dale, A.M., 2013. Neocortical correlates of vibrotactile detection in humans. *J. Cogn. Neurosci.* 25 (1), 49–61.
- Nowak, D.A., Timmann, D., Hermsdörfer, J., 2007. Dexterity in cerebellar agenesis. *Neuropsychologia* 45 (4), 696–703.
- Pavlides, C., Miyashita, E.I.Z.O., Asanuma, H., 1993. Projection from the sensory to the motor cortex is important in learning motor skills in the monkey. *J. Neurophysiol.* 70 (2), 733–741.
- Peelen, M.V., Downing, P.E., 2005. Selectivity for the human body in the fusiform gyrus. *J. Neurophysiol.* 93 (1), 603–608.
- Pilgramm, S., de Haas, B., Helm, F., Zentgraf, K., Stark, R., Munzert, J., Krüger, B., 2016. Motor imagery of hand actions: decoding the content of motor imagery from brain activity in frontal and parietal motor areas. *Hum. Brain Mapp.* 37 (1), 81–93.
- Porter, L.L., White, E.L., 1983. Afferent and efferent pathways of the vibrissal region of primary motor cortex in the mouse. *J. Comp. Neurol.* 214 (3), 279–289.
- Pustina, D., Coslett, H.B., Turkeltaub, P.E., Tustison, N., Schwartz, M.F., Avants, B., 2016. Automated segmentation of chronic stroke lesions using LINDA: lesion identification with neighborhood data analysis. *Hum. Brain Mapp.* 37 (4), 1405–1421.
- Qi, H.X., Jain, N., Collins, C.E., Lyon, D.C., Kaas, J.H., 2010. Functional organization of motor cortex of adult macaque monkeys is altered by sensory loss in infancy. *Proc. Natl. Acad. Sci.* 107 (7), 3192–3197.
- Qi, H.X., Liao, C.C., Reed, J.L., Kaas, J.H., 2019. Reorganization of higher-order somatosensory cortex after sensory loss from hand in squirrel monkeys. *Cereb. Cortex* 29 (10), 4347–4365.
- Rapp, B., Hendel, S.K., Medina, J., 2002. Remodeling of somatosensory hand representations following cerebral lesions in humans. *Neuroreport* 13 (2), 207–211.
- Rehme, A.K., Eickhoff, S.B., Rottschy, C., Fink, G.R., Grefkes, C., 2012. Activation likelihood estimation meta-analysis of motor-related neural activity after stroke. *Neuroimage* 59 (3), 2771–2782.
- Restuccia, D., Valeriani, M., Barba, C., Le Pera, D., Capecci, M., Filippini, V., Molinari, M., 2001. Functional changes of the primary somatosensory cortex in patients with unilateral cerebellar lesions. *Brain* 124 (4), 757–768.
- Rowe, M.J., Turman, A.B., Murray, G.M., Zhang, H.Q., 1996. Parallel processing in somatosensory areas I and II of the cerebral cortex. *Somesthesia Neurobiol. Somatosens. Cortex* 197–211.
- Shadmehr, R., Krakauer, J.W., 2008. A computational neuroanatomy for motor control. *Exp. Brain Res.* 185, 359–381.
- Sultan, F., Augath, M., Hamodeh, S., Murayama, Y., Oeltermann, A., Rauch, A., Thier, P., 2012. Unravelling cerebellar pathways with high temporal precision targeting motor and extensive sensory and parietal networks. *Nat. Commun.* 3 (1), 924.
- Tamè, L., Holmes, N.P., 2016. Involvement of human primary somatosensory cortex in vibrotactile detection depends on task demand. *Neuroimage* 138, 184–196.
- Tamè, L., Pavani, F., Braun, C., Salemme, R., Farnè, A., Reilly, K.T., 2015. Somatotopy and temporal dynamics of sensorimotor interactions: evidence from double afferent inhibition. *Eur. J. Neurosci.* 41 (11), 1459–1465.
- Ter Horst, A. C., Cole, J., Van Lier, R., & Steenbergen, B. (2012). The effect of chronic deafferentation on mental imagery: a case study.
- Touvykine, B., Mansoori, B.K., Jean-Charles, L., Deffeyes, J., Quessy, S., Dancause, N., 2016. The effect of lesion size on the organization of the ipsilesional and contralateral motor cortex. *Neurorehabil. Neural Repair.* 30 (3), 280–292.
- Vingerhoets, G., de Lange, F.P., Vandemaele, P., Deblaere, K., Achter, E., 2002. Motor imagery in mental rotation: an fMRI study. *Neuroimage* 17 (3), 1623–1633.
- Ward, N.S., Brown, M.M., Thompson, A.J., Frackowiak, R.S.J., 2003. Neural correlates of motor recovery after stroke: a longitudinal fMRI study. *Brain* 126 (11), 2476–2496.
- Weeks, R.A., Gerloff, C., Honda, M., Dalakas, M.C., Hallett, M., 1999. Movement-related cerebellar activation in the absence of sensory input. *J. Neurophysiol.* 82 (1), 484–488.
- Weiner, K.S., Grill-Spector, K., 2011. Not one extrastriate body area: using anatomical landmarks, hMT+, and visual field maps to parcellate limb-selective activations in human lateral occipitotemporal cortex. *Neuroimage* 56 (4), 2183–2199.
- West, K.L., Zuppichini, M.D., Turner, M.P., Sivakolundu, D.K., Zhao, Y., Abdelkarim, D., Rypma, B., 2019. BOLD hemodynamic response function changes significantly with healthy aging. *Neuroimage* 188, 198–207.
- Wolpert, D.M., Ghahramani, Z., Jordan, M.I., 1995. An internal model for sensorimotor integration. *Science* 269 (5232), 1880–1882.
- Wong, A.L., Marvel, C.L., Taylor, J.A., Krakauer, J.W., 2019. Can patients with cerebellar disease switch learning mechanisms to reduce their adaptation deficits? *Brain* 142 (3), 662–673.
- Worsley, 2001. Statistical analysis of activation images. In: Jezzard, P., Matthews, P.M., Smith, S.M. (Eds.), Ch 14, in *Functional MRI: An Introduction to Methods*. OUP.
- Xerri, C., Merzenich, M.M., Peterson, B.E., Jenkins, W., 1998. Plasticity of primary somatosensory cortex paralleling sensorimotor skill recovery from stroke in adult monkeys. *J. Neurophysiol.* 79 (4), 2119–2148.
- Yomogida, Y., Sugiura, M., Sassa, Y., Wakusawa, K., Sekiguchi, A., Fukushima, A., Kawashima, R., 2010. The neural basis of agency: an fMRI study. *Neuroimage* 50 (1), 198–207.